Proceedings of the ASME 2020
International Mechanical Engineering Congress & Exposition
IMECE2020
November 16-19, 2020, Portland, OR, USA

IMECE2019-23505

On the design of a DLD-DEP device for separation of circulating tumor cells in blood

Mehdi Rahmati
Mechanical Engineering, Washington State University
Vancouver, WA, USA

Xiaolin Chen
Mechanical Engineering, Washington State University
Vancouver, WA, USA

ABSTRACT

Circulating Tumor Cells (CTCs), which migrate from original sites in a body to distant organs through blood, are a key factor in cancer detection. Emerging Label-free techniques owing to their inherent advantage to preserve characteristics of sorted cells and low consumption of samples can be promising to the prediction of cancer progression and metastasis research. Deterministic Lateral Displacement (DLD) is one of the label-free separation techniques employing a specific arrangement of micro-posts for continuous separation of suspended cells in a buffer based on the size of cells. Separation based solely on size is challenging since the size distributions of CTCs might overlap with those of normal blood cells. To address this problem, DLD can be combined with dielectrophoresis (DEP) technique which is the phenomenon of particle movement in a non-uniform electric field owing to the polarization effect. Although, DLD devices employ the laminar flow in low Reynolds number (Re) fluid flow due to predictability of such flow regimes, they should be improved to work in higher Re flow regime so as to attain high throughput devices. In this paper, a particle tracing simulation is developed to study the effects of different post shapes, shift fraction of micropost arrays, and dielectrophoresis forces on separation of CTCs from peripheral blood cells. Our numerical model and results provide a groundwork for design and fabrication of high-throughput DLD-DEP devices for improvement of CTC separation.

INTRODUCTION

Cancer is one of the most serious diseases threatening human health throughout the world. Based on American Cancer Society report [1], just in 2017 over half a million people died due to cancer in the USA whereas early diagnostisis greatly increases the chance of successful treatment. Tumors excrete cancer cells in blood and other body fluids. The migration of these Circulating Tumor Cells (CTCs) from original sites to distant organs through blood is the main reason of death since CTCs are responsible for initiating the metastasis. CTCs are a key factor in cancer detection, however their extreme rarity in bloodstreams makes it challenging to separate them. The link between cancer metastasis and CTCs has made the investigation of CTCs significant for applications such as early detection of cancer and therapeutics. Hence, in recent years, a large volume of studies has been carried out to develop methods of CTC separation from other cells within the bloodstream.

Tremendous advances in microfluidics and microfabrication technologies have led to the development of many new devices for the characterization and sorting of single cells with no need of exogenous labels. Label-free microfluidics reduce preparation time and cost of conventional methods working based on fluorescent or magnetic labels. Moreover, these devices enable analysis of cell properties such as mechanical phenotype and dielectric parameters that cannot be characterized with traditional labels [2]. Various cell properties are utilized for label-free cell sorting such as size [3-5], dielectric characteristics [6, 7], and coupling multi-properties [8]. One of the most common label-free separation techniques is the Deterministic Lateral Displacement (DLD), which has indicated as a potential capability to separate particles and cells of different sizes. This technique uses a specific arrangement of micro-posts for continuous separation of suspended particles/cells in a buffer based on the critical size of particles/cells [9]. For the first time, Huang et al. [10] presented DLD technique as an effective separation approach for sorting of microspheres of 0.8, 0.9, and 1.0 micrometers in 40 seconds with a resolution about10 nanometers, which was better than the time and resolution of conventional flow techniques.

Although most of DLD devices work with a creeping flow regime with a Reynolds (Re) number much less than 1, due to the extreme rarity of CTCs in blood samples, a large

volume of blood samples should be processed leading to an increase in the process time to find and sort CTCs effectively. Accordingly, it is crucial to investigate high throughput DLD microchips so as to maximize the chances of finding the CTCs and minimize the process time. For example, Lubbersen et al. [11] studied the influence of moderately high Reynolds numbers on the performance of DLD devices. Their results showed an efficiency improvement in sorting of 234 μm and 441 μm polystyrene particles at high flow rates (Re=18).

Due to the fact that DLD method works based on critical diameter of particles, it may suffer from the overlap between CTC size and cell size. However, this issue can be addressed using dielectrophoresis (DEP) technique. It has been demonstrated that irrespective of cancer types, the dielectric characteristics of CTCs differ significantly from peripheral blood cells, resulting in noticeable sorting accuracy [12]. In general, insulator-based [13] and electrode-based [14] dielectrophoresis are the two common ways to generate a nonuniform electric field. Compared to insulator-based dielectrophoresis, electrode-based dielectrophoresis is disadvantageous owing to electrodes' fouling, and bubble formation in the channel and so forth. Hence, insulator-based dielectrophoresis (iDEP) is employed in this study. Insulator-based dielectrophoresis (iDEP) makes a nonuniform electric field utilizing the electrodes installed outside the microchip channel and the embedded insulating posts inside the channel [15].

Even though the literature is replete studies regarding DLD devises [16-19], just a few investigations have been published about DLD-DEP devices. To the best of author's knowledge, there is no report in the literature to investigate the influences of elliptical post on the separation of CTCs from peripheral blood cells in DLD-DEP devices. Therefore, in the present research, a numerical model is developed using the particle tracing module of COMSOL Multiphysics to investigate the effects of elliptical post, shift fraction of microposts arrays, dielectrophoresis force and electric field norm on the performance of DLD-DEP devices and subsequently to provide a groundwork for designers.

THEORY & SIMULATION

Deterministic lateral displacement (DLD)

DLD separation technique is a size-based separation technique using tilted arrays of microposts to separate particles. As depicted in Figure 1, the microposts placed in a channel make different streamline in the fluid flow [5]. The width of the first streamline near the post determines the particle's motion mode. In more details, particles with a diameter less than twice of the first streamline, called critical diameter (Dc), remain in the same streamline and follow a zigzag motion mode while particles with a diameter greater than the critical diameter displace laterally and follow a bumped motion mode (see Figure 1).

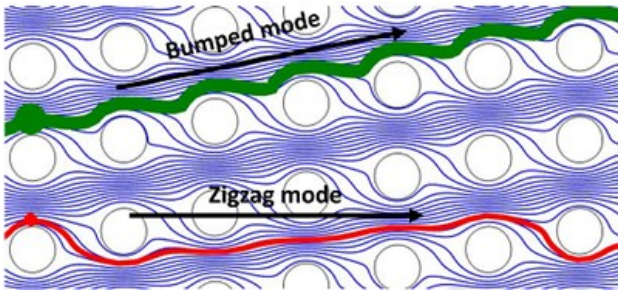

Figure 1. Illustration of bumped and zigzag modes in a DLD device.

Inglis et al. [20] presented a theoretical approach to derive a formula for critical diameter of DLD devices with circular posts as follows:

$$D_C = \mathrm{g}\left[1 + 2w + \frac{1}{2w}\right] \quad (1)$$

where g denotes the gap size between posts and w is determined from the equation (2)

$$w^3 = \frac{1}{8} - \frac{\varepsilon}{4} \pm \sqrt{\frac{\varepsilon}{16}(\varepsilon - 1)} \quad (2)$$

in this equation, ε is row shift fraction which indicates the slope of the post arrays and is defined as $\frac{\Delta\lambda}{\lambda}$ where $\Delta\lambda$ denotes the shifted distance between microposts and λ is the distance from center to center of adjacent microposts as shown in Figure 2.

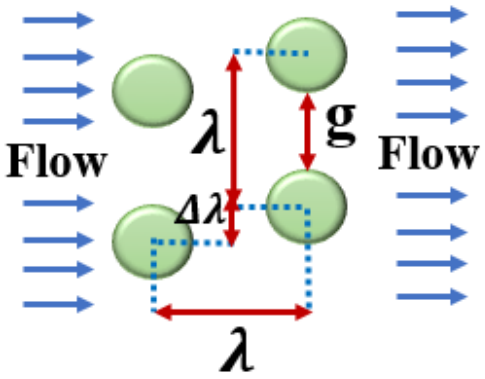

Figure 2. Geometrical parameters of DLD post arrays.

Dielectrophoresis

When a cell is in a non-uniform electric field, it may be polarized and experiences a force from the electric field which this phenomenon is called Dielectrophoresis (DEP). Dielectrophoresis separation method uses the difference between dielectric properties of different cells. The time average of the DEP force is express as [21]:

$$< \boldsymbol{F_{DEP}}(t) >= 2\pi\mu_m r^3 Re[K_{CM}(\omega)]\nabla|\boldsymbol{E_{rms}}|^2 \quad (3)$$

where μ_m and r are permittivity of the medium and radius of cells, respectively. $Re(K_{CM})$ refers to the real part of the Clausius-Mossotti factor defined as [21]:

$$K_{CM}(\omega) = \frac{\bar{\mu}_{cell} - \bar{\mu}_m}{\bar{\mu}_{cell} + 2\bar{\mu}_m} \quad (4)$$

in which $\bar{\mu} = \mu - j\frac{\sigma}{\omega}$ denotes the complex permittivity considering angular frequency (ω), the conductivity (σ) and permittivity (μ) of the cell and the medium. If the cell is more polarizable than the medium, a positive DEP force can be applied to the cell that attracts it to the high electric field regions. On the other hand, if the medium is more polarizable than the cell, a negative DEP force can be applied to the cell that repels it from high electric field regions. Furthermore, the real part of Clausius-Mossotti factor can be equal to zero for a certain value of applied frequency ω called crossover frequency. When frequency of electric field is equal to the crossover frequency of a specific cell, no DEP force applies to the cell whereas positive or negative forces might be applied to the other kinds of cells.

Computational Model Description

As illustrated in Figure 3, the DLD-DEP device consists of microposts arrays placed in the flow direction and external AC electric field is aligned to be parallel with fluid flow. The device has two inlets which one of them is for flowing the sample through the device and another one is for running the buffer. The reason for the use of the buffer is to dilute the sample and to provide sufficient flow rate for the system to work effectively as well as to concentrate the flow of cells to enter to the specific positions of the DLD arrays. In addition, two outlets are placed at the end of the device to collect separated CTCs and the rest of blood sample.

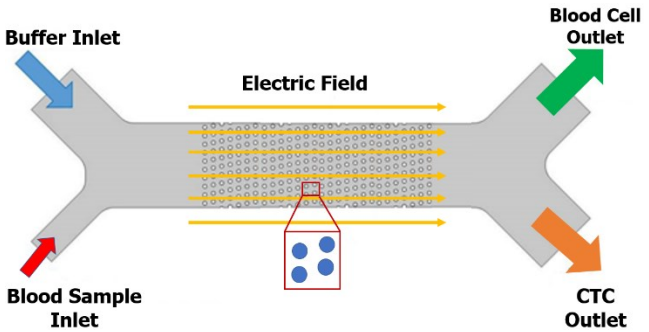

Figure 3. Model geometry of the DLD-DEP device.

In this article, two devices are investigated; one of them with circular posts another one with elliptical posts. In both devices, the gap size between posts (g) is 40 μm and diameter of circular and elliptical posts are 40 μm and 40×20 μm, respectively. In addition, external electric field is aligned to be parallel with fluid flow, whereas the row shift fraction (ε) is considered as a design variable.

As mentioned above, coupled DLD-DEP separation technique works based on coupling effect of fluid and electric fields. The flow field can be determined by solving the continuity and Navier-Stokes equations:

$$\rho\left[\frac{\partial \boldsymbol{v}}{\partial t} + \boldsymbol{v}.\nabla\boldsymbol{v}\right] = -\nabla p + \eta\nabla^2\boldsymbol{v} \quad (5)$$

$$\nabla.\mathbf{v} = 0 \quad (6)$$

where ρ, $\boldsymbol{v}$, p, and η are fluid density, velocity vector, pressure, and viscosity, respectively.

On the other hand, the electric field $\boldsymbol{E}$ can be determined by charge conservation and Gauss's law which the governing equations are presented as follows:

$$\nabla \cdot (\sigma\boldsymbol{E}) + \frac{\partial \rho_f}{\partial t} = 0 \quad (7)$$

$$\nabla \cdot (\mu_m\boldsymbol{E}) = \rho_f \quad (8)$$

$$\boldsymbol{E} = -\nabla\phi \quad (9)$$

where $\boldsymbol{E}$ and t are electric field and time, respectively. ρ_f indicates the free charge density, σ is the medium conductivity. μ_m denotes the medium permittivity and ϕ is the electric potential.

In this Study, COMSOL Multiphysics (Fluid Flow and AC/DC modules) is employed to solve the mentioned equations in the system domain and consequently to use particle tracing module to simulate trajectory of the cells under the net forces on them. In more details, this module models the cell transport within the domain using Newton's second law which relates the net forces on the cell to its rate of momentum changes in an inertial reference frame as represented in equation (10).

$$\frac{d}{dt}(m_{cell}\boldsymbol{v_{cell}}) = \boldsymbol{F_{Drag}} + \boldsymbol{F_{DEP}} \quad (10)$$

where m_{cell} and $\boldsymbol{v_{cell}}$ are the cell mass and the cell velocity, respectively. $\boldsymbol{F_{Drag}}$ and $\boldsymbol{F_{DEP}}$ denote drag and dielectroporetic forces which can be determined by equations (11) and (3), respectively. It is worth mentioning that the impacts of gravity and buoyancy forces on the cells are assumed to be negligible. Moreover, Stokes drag law is employed in this study to calculate the drag force applied on the cells which is represented as follows

$$\boldsymbol{F_{Drag}} = 6\mu r_{cell}\pi(\boldsymbol{v} - \boldsymbol{v_{cell}}) \quad (11)$$

where μ indicates the fluid viscosity, r_{cell} is the cell radius, $\boldsymbol{v}$ and $\boldsymbol{v_{cell}}$ denote the velocities of the fluid and the cell, respectively.

RESULTS AND DISCUSSION

In this section, the numerical model is validated and then simulation results and the effects of electric field, post shape and row shift fraction are discussed in details.

Validation

In order to examine the accuracy of the numerical model, the fluid flow field was solved in the domain in the absence of the electric field. Using particle tracing module, particles with different diameter sizes were injected into the DLD device to determine the critical diameter of the DLD arrays for various row shift fractions (ε) in Stokes flow regime. Figure 4, depicts the comparison between the results of numerical model and those obtained from equation (1). This figure shows that there is a good agreement between DLD critical diameters obtained by the theoretical formula and the numerical simulations specifically for low values of ε.

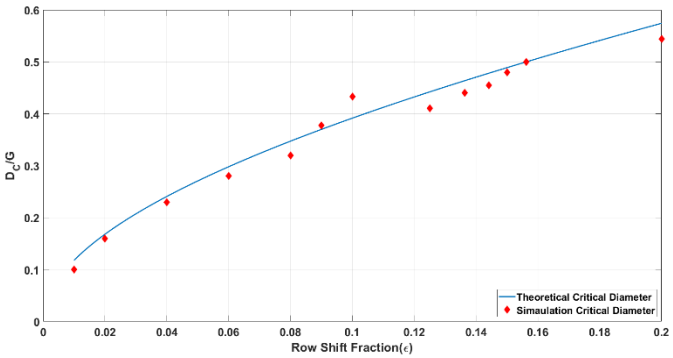

Figure 4. Comparison of the DLD critical diameter obtained by theoretical and numerical methods versus different values of $\boldsymbol{\varepsilon}$.

As mentioned above, dielectric properties of cells and the medium as well as the frequency of the applied electric field affect the real part of Clausius-Mossotti factor and consequently can determine whether the cells experience positive, negative, or zero DEP forces. Hence, the difference in the intrinsic properties of various cells can address the problem of the cell separation by selecting appropriate frequencies. In this study, Granulocytes and MDA-231 breast cancer cells were selected as representatives of WBCs and CTCs to determine the input parameters of the numerical model. The membrane thickness of both cells is considered to be 4 *nm*. In addition, diameter of WBCs is assumed to be 10 μm while two diameter sizes of 10 μm and 14 μm are considered for CTCs. Table 1 presents electrical properties of the mentioned cells [22, 23].

In order to compare the dielectric behavior of the cells in an electrical field, the variation of Classius-Mossoti factor for both cells is obtained in a medium (buffer) with electrical conductivity of 0.05 *S/m*, and the results are shown in Figure 5. This figure helps us to predict the behavior of the cells and consequently separate them by choosing an appropriate frequency. It can be seen from this figure that the crossover frequency of CTCs is lower than the crossover frequency of WBCs. Therefore, adjusting the electric field frequency to the crossover frequency of CTCs leads to a zigzag mode for CTCs and a bumped mode for WBCs and consequently a successful separation of cells. Even though Figure 1 has been drawn for specific type of CTCs, it has been demonstrated that the crossover frequency of all types of NCI-60 cancer cell line panel is lower than crossover frequency of blood cells [24]. Therefore, similar approach can be employed for the separation of other kinds of CTCs from blood.

Table 1. Electrical properties of the cells.

Cell type	Tissue type	ε_{mem}	σ_{mem} (S/m)	ε_{cyt}	σ_{cyt} (S/m)
Granulocytes (WBC)	Blood	5	1×10^6	65	0.6
MDA-231	Breast	11.75	1×10^6	52	0.62

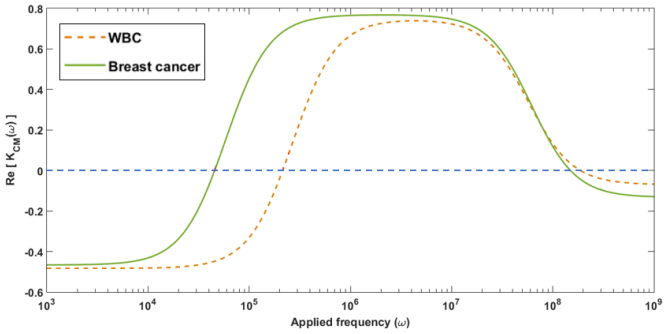

Figure 5. The real part of Clausius-Mossotti factor for MDA-231 CTCs and WBCs in a medium with conductivity of 0.05 *S/m* versus different applied frequencies.

A nonuniform electric field is necessary for the manipulation of the cells. Figure 6 shows a nonuniform electric field made by the DLD arrays of circular and elliptical insulators. In both arrangements, low electric field regions are placed at the trailing and leading edges of the microposts whereas high electric regions are placed at the lower and upper edges. A DLD-DEP device works based on the competition between the dielectrophoretic and drag forces applied on the cells; thus, the resultant of these forces determines the direction of the cells.

This proposed DLD-DEP device is designed so that critical size of the device is larger than the diameter of the biggest CTCs and WBCs; thus, in the absence of the electric field, both CTCs and WBCs traverse with a zigzag mode while in the presence of the electric field which its frequency is equal to crossover frequency of CTCs, WBCs and CTCs follow bumped and zigzag modes, respectively, because WBCs and CTCs experience negative DEP and zero DEP forces, respectively. In more details, by applying electric field, WBCs tend to be repelled from high electric field regions and attracted to the lower regions; thus, high electric field regions should be

strong enough to repel the WBCs effectively from the post to be placed on the main stream with a bumped mode.

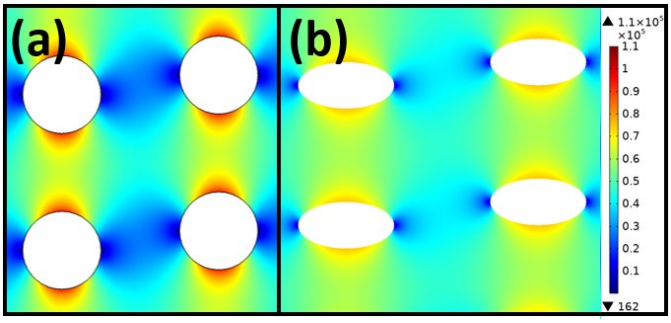

Figure 6. Comparison of electric field around circular and elliptical posts.

Figure 7 and 8 show simulation results of particle tracing in two DLD-DEP devices with circular and elliptical post shapes, respectively. Red, blue and green particles represent WBCs, small and big CTCs with diameters of 10 μm, 10 μm and 14 μm, respectively.

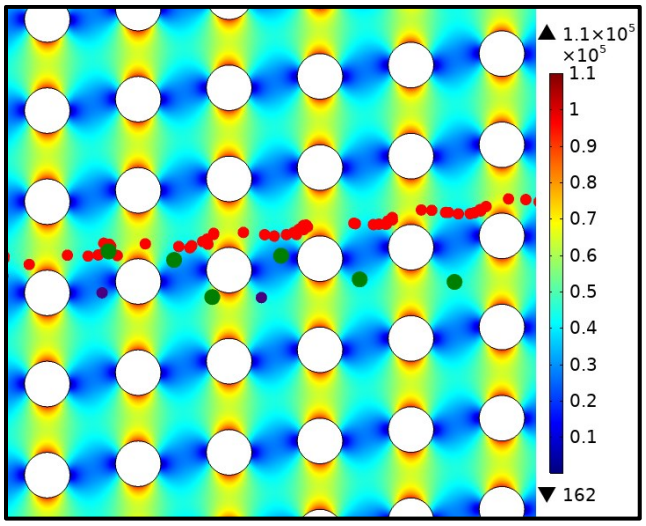

Figure 7. Trajectory of WBCs and CTCs when applied frequency is equal to crossover frequency of CTCs in a DLD-DEP device with circular posts.

Even though in both simulations, the row shift fraction is equal to 1/8, and both DLD-DEP devices work with applied electric potential of 25V, and flow velocity of 350 $\mu m/s$, a successful separation is observed just for the device with circular posts. In other words, for the device with elliptical posts, the WBCs stick to the leading edges of the posts which is due to the fact that variation of the electric field is smaller around the elliptical posts compared to the circular posts; hence, norm of the electric field on the upper edges is not high enough to repel the WBCs effectively from the posts and place them on the main stream with a bumped mode. However, CTCs are unaffected by the nonuniform electric field and follow a zigzag mode.

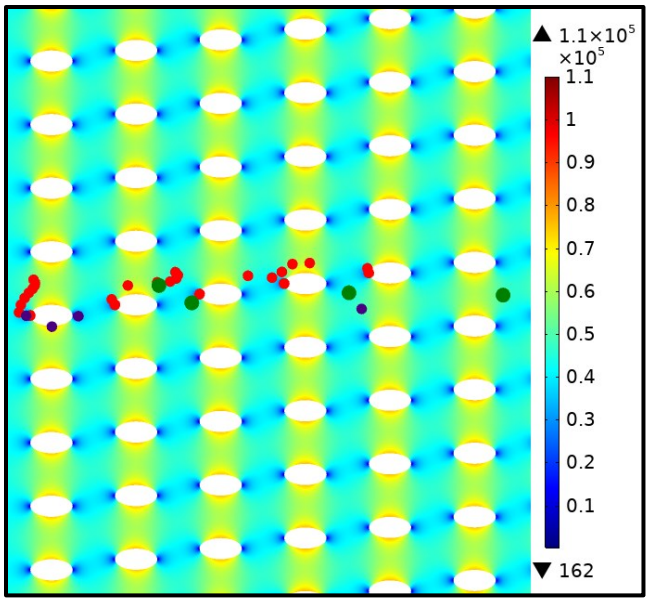

Figure 8. Trajectory of WBCs and CTCs when applied frequency is equal to crossover frequency of CTCs in a DLD-DEP device with elliptical posts.

One of the advantages of continuous separation of CTCs is an increase in viability of the cells compared to the cell trapping method. Another problem of trapping WBCs is device clogging which leads to device failure. Hence, in the next part, the effects of post shapes, row shift fraction and on the continuous separation of CTCs are investigated to find the suitable ranges of flow velocity and electric field norm at different DLD array configurations.

Figures 9 and 10 illustrate the possible electric field and flow velocity for pushing the WBCs into a bumped mode at different row shift fractions for DLD-DEP devices with circular and elliptical posts, respectively. It should be noted that the gap size between the posts and size of the devices are fixed in this study. The results indicate that for both circular and elliptical posts, trajectory of the WBCs can change from zigzag to bumped mode for row shift fractions with the range between 1/8 to 1/10. Interestingly, at higher row shift fractions and under any flow velocities and electric field norm, WBCs tend to be trapped in the lower electric field regions at leading edges of the posts. Its reason is that the influence of low electric field regions raises at higher values of the row shift fraction.

It can be seen from Figures 9 and 10 that at each specific value of electric field norm, there exist lower and upper limits for possible flow velocities. In addition, choosing velocity values lower than this range leads to cell trapping at low electric field areas due to DEP force dominancy while exceeding the velocity range results in a zigzag mode for WBCs owing to drag force dominancy. It is noteworthy to mention that points A and B on Figures 9 and 10 show the working conditions of DLD-DEP devices presented in Figures 7 and 8, respectively. By comparing Figures 9 and 10, it can be perceived that at each specific value of electric field norm, both lower and upper limits of possible velocities corresponding to elliptical posts are

higher than those of circular posts. It means that DLD-DEP devices with elliptical posts are more appropriate for high flow velocities or moderately high Re regime whereas those with circular posts are more suitable for low flow velocities since variation of the electric field is smaller around the elliptical posts compared to the circular posts. Hence, norm of the electric field on the upper edges of the elliptical posts is not high enough to repel the WBCs effectively from the posts and place them on the main stream with a bumped mode.

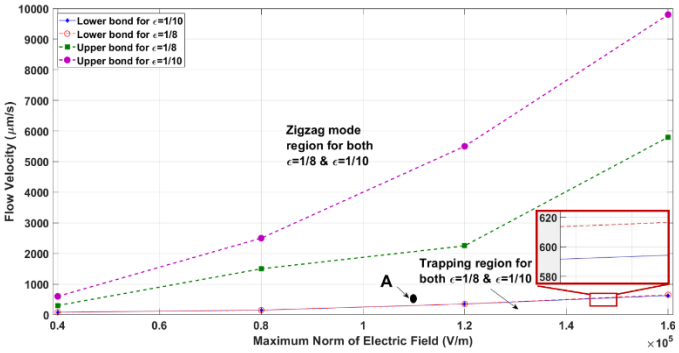

Figure 9. Lower and upper limits of the flow velocity versus electric field norm at different row shift fractions for the DLD-DEP device with circular posts.

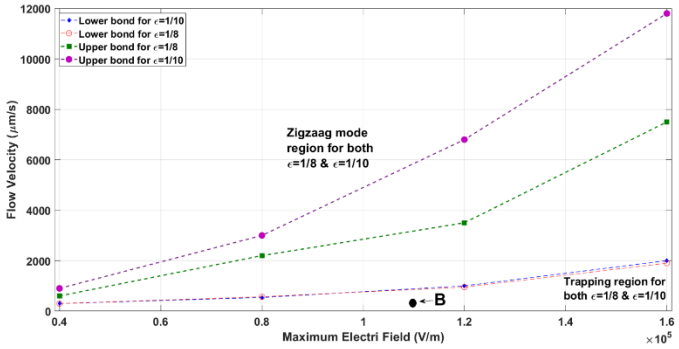

Figure 10. Lower and upper limits of the flow velocity versus electric field norm at different row shift fractions for the DLD-DEP device with elliptical posts.

CONCLUSIONS

In this article, a numerical model was developed using the particle tracing module of COMSOL Multiphysics to investigate the effects of different post shapes, shift fraction of micropost arrays, and dielectrophoresis forces on the performance of DLD-DEP devices. In order to validate the model, critical diameters of the DLD device obtained for different shift fraction in the absence of electric field were compared with a theoretical formula. Lower and upper limits of the flow velocity for different values of electric field norm and row shift fraction were obtained for both DLD-DEP devices with circular and elliptical posts. Our results indicate that DLD-DEP devices with elliptical posts are more appropriate for high flow velocities or moderately high Re regime whereas those with circular posts are more suitable for low flow velocities since variation of the electric field is smaller around the elliptical posts compared to the circular posts. Hence, norm of the electric field on the upper edges of the elliptical posts is not high enough to repel the WBCs effectively from the posts and place them on the main stream with a bumped mode. Moreover, for both circular and elliptical posts, trajectory of the WBCs can change from zigzag to bumped mode for row shift fractions with the range between 1/8 to 1/10. Finally, it is concluded that combination of DLD with DEP introduces a powerful technique for separation of CTCs from peripheral blood cells.

REFERENCES

[1] Siegel, R.L., Miller, K.D., Fedewa, S.A., Ahnen, D.J., Meester, R.G., Barzi, A. and Jemal, A., 2017. Colorectal cancer statistics, 2017. *CA: a cancer journal for clinicians*, *67*(3), pp.177-193.

[2] Carey, T. R., Cotner, K. L., Li, B., Sohn, L. L., 2019. Developments in label-free microfluidic methods for single-cell analysis and sorting. Wiley Interdisciplinary Reviews: *Nanomedicine and Nanobiotechnology*, 11(1), e1529.

[3] Dincau, B. M., Aghilinejad, A., Hammersley, T., Chen, X., & Kim, J. H., 2018. Deterministic lateral displacement (DLD) in the high Reynolds number regime: high-throughput and dynamic separation characteristics. *Microfluidics and Nanofluidics*, 22(6), 59.

[4] Aghilinejad, A., Aghaamoo, M., Chen, X., 2019. On the transport of particles/cells in high-throughput deterministic lateral displacement devices: Implications for circulating tumor cell separation. *Biomicrofluidics*, 13(3), 034112.

[5] Dincau, B.M., Aghilinejad, A., Chen, X., Moon, S.Y. and Kim, J.H., 2018. Vortex-free high-Reynolds deterministic lateral displacement (DLD) via airfoil pillars. *Microfluidics and Nanofluidics*, *22*(12), p.137.

[6] Aghilinejad, A., Aghaamoo, M., Chen, X. and Xu, J., 2018. Effects of electrothermal vortices on insulator-based dielectrophoresis for circulating tumor cell separation. *Electrophoresis*, *39*(5-6), pp.869-877.

[7] Aghaamoo, M., Aghilinejad, A., Chen, X., 2017, February. Numerical study of insulator-based dielectrophoresis method for circulating tumor cell separation. In *Microfluidics, BioMEMS, and Medical Microsystems XV* (Vol. 10061, p. 100611A). International Society for Optics and Photonics.

[8] Aghilinejad, A., Aghaamoo, M., Chen, X., 2017, November. Numerical Study of Joule Heating Effect on Dielectrophoresis-Based Circulating Tumor Cell Separation. In *ASME 2017 International Mechanical Engineering Congress and Exposition* (pp. V003T04A014-V003T04A014). American Society of Mechanical Engineers.

[9] Salafi, T., Zhang, Y., Zhang, Y. 2019. A Review on Deterministic Lateral Displacement for Particle Separation and Detection. *Nano-Micro Letters*, 11(1), 77.

[10] Huang, L.R., Cox, E.C., Austin, R.H. and Sturm, J.C., 2004. Continuous particle separation through deterministic lateral displacement. *Science*, *304*(5673), pp.987-990.

[11] Lubbersen, Y.S., Schutyser, M.A.I. and Boom, R.M., 2012. Suspension separation with deterministic ratchets at moderate Reynolds numbers. *Chemical engineering science*, *73*, pp.314-320.

[12] Shim, S., Stemke-Hale, K., Noshari, J., Becker, F. F., Gascoyne, P. R., 2013. Dielectrophoresis has broad applicability to marker-free isolation of tumor cells from blood by microfluidic systems. *Biomicrofluidics*, 7(1), 011808.

[13] Srivastava, S. K., Gencoglu, A., & Minerick, A. R., 2011. DC insulator dielectrophoretic applications in microdevice technology: a review. *Analytical and bioanalytical chemistry*, 399(1), pp.301-321.

[14] Khoshmanesh, K., Nahavandi, S., Baratchi, S., Mitchell, A., Kalantar-zadeh, K., 2011. Dielectrophoretic platforms for bio-microfluidic systems. *Biosensors and Bioelectronics*, 26(5), 1800-1814.

[15] Aghaamoo, M., Aghilinejad, A., Chen, X. and Xu, J., 2019. On the design of deterministic dielectrophoresis for continuous separation of circulating tumor cells from peripheral blood cells. *Electrophoresis*, 40(10), pp.1486-1493.

[16] Aghilinejad, A., Aghaamoo, M. and Chen, X., 2017, November. Numerical Study of Joule Heating Effect on Dielectrophoresis-Based Circulating Tumor Cell Separation. In *ASME 2017 International Mechanical Engineering Congress and Exposition* (pp. V003T04A014-V003T04A014). American Society of Mechanical Engineers.

[17] Zhang, X., Hashem, M.A., Chen, X. and Tan, H., 2018. On passing a non-Newtonian circulating tumor cell (CTC) through a deformation-based microfluidic chip. *Theoretical and Computational Fluid Dynamics*, *32*(6), pp.753-764.

[18] Jusková, P., Matthys, L., Viovy, J.L. and Malaquin, L., 2020. 3D deterministic lateral displacement (3D-DLD) cartridge system for high throughput particle sorting. *Chemical Communications*, 56(38), pp.5190-5193.

[19] Calero, V., Garcia-Sanchez, P., Ramos, A. and Morgan, H., 2020. Electrokinetic biased Deterministic Lateral Displacement: Scaling Analysis and Simulations. *Journal of Chromatography A*, p.461151.

[20] Inglis, D. W., Davis, J. A., Austin, R. H., Sturm, J. C., 2006, Critical particle size for fractionation by deterministic lateral displacement. *Lab on a Chip*, 6(5), pp.655-658.

[21] Jones, T. B., Electromechanics of Particles, Cambridge University Press, Cambridge 1995.

[22] Yang, J., Huang, Y., Wang, X., Wang, X.B., Becker, F.F. and Gascoyne, P.R., 1999. Dielectric properties of human leukocyte subpopulations determined by electrorotation as a cell separation criterion. *Biophysical journal*, 76(6), pp.3307-3314.

[23] Becker, F. F., Wang, X. B., Huang, Y., Pethig, R., Vykoukal, J., & Gascoyne, P. R., 1995, Separation of human breast cancer cells from blood by differential dielectric affinity, *Proceedings of the National Academy of Sciences*, 92(3), pp. 860-864.

[24] Gascoyne, P.R., Shim, S., Noshari, J., Becker, F.F. and Stemke-Hale, K., 2013. Correlations between the dielectric properties and exterior morphology of cells revealed by dielectrophoretic field-flow fractionation. *Electrophoresis*, 34(7), pp.1042-1050.